IOPscience iopscience.iop.org

Home Search Collections Journals About Contact us My IOPscience

Gonioreflectometric properties of metal surfaces

This content has been downloaded from IOPscience. Please scroll down to see the full text.

2014 Metrologia 51 S314

(http://iopscience.iop.org/0026-1394/51/6/S314)

View the table of contents for this issue, or go to the journal homepage for more

Download details:

IP Address: 130.233.110.57
This content was downloaded on 21/11/2014 at 11:32

Please note that terms and conditions apply.

IOP Publishing | Bureau International des Poids et Mesures Metrologia
Metrologia 51 (2014) S314–S318 doi:10.1088/0026-1394/51/6/S314

Gonioreflectometric properties of metal surfaces

P Jaanson[1,2], F Manoocheri[1,2], H Mäntynen[1], M Gergely[3], J-L Widlowski[3] and E Ikonen[1,2]

[1] Metrology Research Institute, Aalto University, Espoo, Finland
[2] Centre for Metrology and Accreditation (MIKES), Espoo, Finland
[3] European Commission DG Joint Research Centre, Ispra, Italy

E-mail: priit.jaanson@aalto.fi

Received 9 June 2014, revised 21 August 2014
Accepted for publication 22 August 2014
Published 20 November 2014

Abstract

Angularly resolved measurements of scattered light from surfaces can provide useful information in various fields of research and industry, such as computer graphics, satellite based Earth observation etc. In practice, empirical or physics-based models are needed to interpolate the measurement results, because a thorough characterization of the surfaces under all relevant conditions may not be feasible. In this work, plain and anodized metal samples were prepared and measured optically for bidirectional reflectance distribution function (BRDF) and mechanically for surface roughness. Two models for BRDF (Torrance–Sparrow model and a polarimetric BRDF model) were fitted to the measured values. A better fit was obtained for plain metal surfaces than for anodized surfaces.

Keywords: BRDF, modelling, aluminium, anodized, reflectance

(Some figures may appear in colour only in the online journal)

1. Introduction

Satellite based observation of Earth in the visible and near-infrared wavelength range can provide crucial information to study climate change. In order to interpret the measured data a variety of radiative transfer (RT) codes have been developed, which simulate the propagation of radiation within different geophysical media (e.g. the atmosphere, the oceans and the biosphere) by transmission, absorption and scattering [1]. Considerable effort is put into validation of these RT codes, one approach focusing on SI traceability using artificial targets is described in [2]. Many RT codes make use of models describing the light scattering from surfaces. The scattered light from a surface is usually described by a bidirectional reflectance distribution function (BRDF), which is defined as

$$f(\Omega_i, \Omega_r) = \frac{\mathrm{d}L_r(\Omega_i, \Omega_r)}{\mathrm{d}E_i(\Omega_i)}, \qquad (1)$$

where $\mathrm{d}L_r$ is the radiance of the sample in the direction Ω_r while illuminated by irradiance $\mathrm{d}E_i$ from the direction Ω_i. Due to many parameters associated with the BRDF, the measurements of real surfaces can be time consuming. In order to save measurement time, various BRDF models have been developed mainly based on either geometrical optics or wave optics [3–5]. The results of measurements for plain and anodized aluminium surfaces can then be compared with the calculated values, for example from the Torrance–Sparrow BRDF model [3, 4, 6] or from the polarimetric BRDF model [5].

In this paper methods are developed to analyse the reflectance data of RT code validation artefacts consisting of several small cubes [2]. The topographic and optical properties of these artefacts have been characterized by traceable measurements. The calculated reflectance of the artefacts can be derived on the basis of gonioreflectometric properties of the individual cube surfaces. As a conclusion of this work, BRDF models of the individual surfaces for obtaining the calculated reflectance of RT code validation artefacts are recommended and the limits of performance of the BRDF models are assessed.

2. Materials and methods

2.1. Samples

Two types of metal surfaces have been produced: roughened plain aluminium and roughened aluminium anodized with a

 © 2014 BIPM & IOP Publishing Ltd Printed in the UK

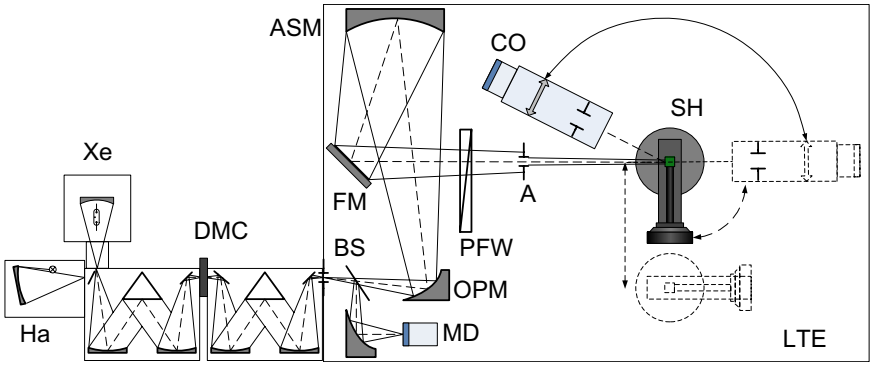

Figure 1. MIKES-Aalto gonioreflectometer. Xe–xenon arc lamp, Ha–halogen lamp, DMC–double monochromator, BS–beam splitter, MD–monitor detector, OPM–off-axis parabolic mirror, ASM–aspherical mirror, FM–flat mirror, PFW–polarizer filter wheel, A–aperture, CO–collection optics, LTE–light tight enclosure, SH–sample holder.

green pigment. The surfaces have been characterized for BRDF and surface roughness.

The samples are cubes made out of 7075 aluminium alloy with a nominal 12 mm edge length. Five visible surfaces of the cubes were roughened by abrasive blasting. In order to avoid the edges from rounding, the process was performed for multiple samples at once, with the sides of the cubes tightly adjacent to each other. Some of the roughened cubes were anodized using a green pigment.

Table 1. List of symbols for equations (2)–(5).

Symbol	Definition
θ_p	half angle between incident and viewing direction
η	complex index of refraction
$(\theta_i, \phi_i; \theta_r, \phi_r)$	zenith and azimuth angles for incident (i) and reflected (r) light
$(\Omega_i, \Omega_L, \Omega_r)$	shortened notation for the direction of incident light (i), local surface normal (L), direction of reflected light (r)

2.2. Instruments

The measurements of BRDF have been carried out with the MIKES-Aalto gonioreflectometer [7]. The instrument is designed to perform angularly resolved spectrophotometric measurements. The source system and the beam guiding optics are described in figure 1. The sample area contains a linear translator for spatial uniformity measurements and a turntable to adjust the angle of incident light on the sample. The sample holder comprises two automatic goniometers to allow measurement of all visible surfaces of the cube sample. The collection system consists of a precision aperture, lens, a silicon photodetector and a low noise current preamplifier. The detector is mounted on a goniometer allowing the movement of the detector by nearly 360° around the sample. The polarization is controlled only on the incident beam.

2.3. Measurements

2.3.1. Form and surface roughness. Measurements of surface roughness and form of the cubes have been carried out with a form measuring machine. The form measuring machine has a contact stylus with a nominal radius of 2 µm and contact force of 1 mN. The cube edges had a radius of curvature of approximately 70 µm. In addition to form, surface roughness parameters have also been evaluated from the height profiles measured in three lines across every surface.

2.3.2. BRDF measurements. The BRDFs of surfaces have been measured in the plane of incidence with the illumination zenith angles ranging from 0° to 60° and the viewing zenith angles ranging from −60° to 80°. A tungsten–halogen lamp was used for the measurements and the wavelength of light was 525 nm and the bandwidth 5 nm. The measurements were conducted for both s- and p-polarized incident light. The BRDF for unpolarized light is evaluated on the basis of s- and p-polarized reflectance data. The distance of the precision aperture of diameter 24.995(5) mm from the sample is 471.15(20) mm, which makes the solid angle of collection equal to 2.210(2) msr.

2.4. Models

2.4.1. Torrance–Sparrow model. The Torrance–Sparrow (T–S) model is a geometrical optics based BRDF model which approximates a rough surface with randomly oriented mirror like micro facets [3]:

$$f_\mathrm{TS}(\theta_i, \phi_i; \theta_r, \phi_r) = \frac{1}{\pi}\left[D(\theta_i) + S\frac{F(\theta_\mathrm{p}, \eta)T(\Omega_i, \Omega_\mathrm{L}, \Omega_r)A(\Omega_i, \Omega_\mathrm{L}, \Omega_r)}{4\cos(\theta_i)\cos(\theta_r)}\right]. \quad (2)$$

The BRDF is expressed by two terms: a Lambertian diffuse component D and a specular component comprising the weight S, Fresnel reflection F, the surface self-shadowing coefficient A described by Blinn [8] and the micro facet orientation probability T, which is given by the Beckmann distribution [4]. The rest of the symbols are given in table 1.

2.4.2. Polarimetric BRDF model. The polarimetric BRDF model (pBRDF) used in this work is adapted from the model described by Hyde and Schmidt in [5]. The model is based

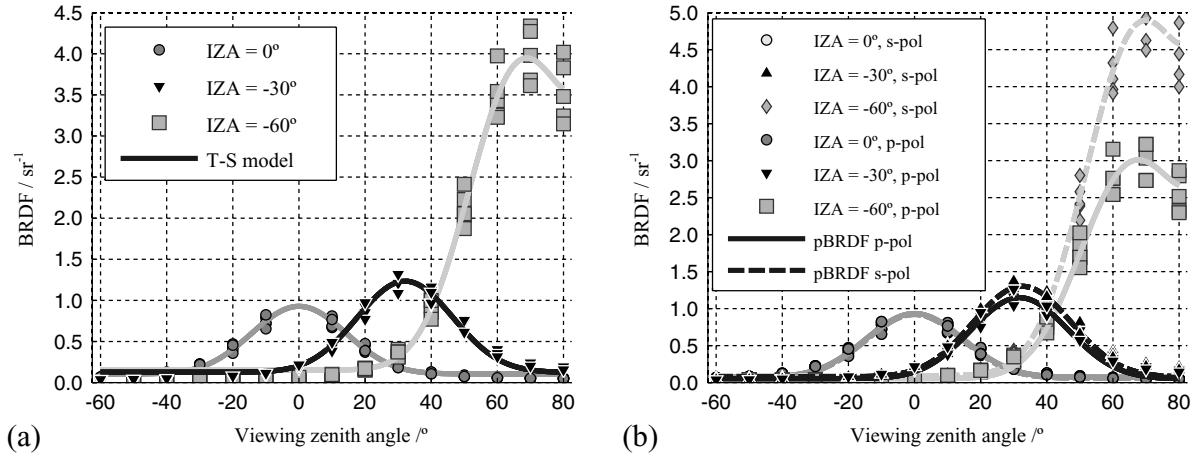

Figure 2. Measurement results of five plain aluminium surfaces and calculated curves for one surface by (*a*) T–S model, $R^2 = 0.999$, and (*b*) pBRDF model, $R^2 = 0.998$. IZA is the illumination zenith angle. Negative viewing zenith angles correspond to the direction of incident light.

on the T–S model. The differences as compared with the T–S model are that Mueller calculus [9] is used to describe the polarization state of the incident and reflected light and that the diffuse component is limited to preserve the conservation of energy.

The full polarimetric BRDF model description can be found in [5] and [10]. Due to the performed measurements, only the unpolarized component of the BRDF function is expressed here:

$$f_{\mathrm{HS}}(\theta_i, \phi_i; \theta_r, \phi_r) = r\frac{1}{\pi}\left(D_{\mathrm{HS}} + S_{\mathrm{HS}}\right), \tag{3}$$

$$D_{\mathrm{HS}} = M_{00}(\beta, \eta) \times \left[1 - \int_0^{2\pi}\int_0^{\pi/2} S_{\mathrm{HS,PR}}\cos(\theta_r)\sin(\theta_r)\mathrm{d}\theta_r\mathrm{d}\phi_r\right], \tag{4}$$

$$S_{\mathrm{HS}} = \frac{M_{00}(\beta, \eta)T(\Omega_i, \Omega_{\mathrm{L}}, \Omega_r)A(\Omega_i, \Omega_L, \Omega_r)}{4\cos(\theta_i)\cos(\theta_r)}. \tag{5}$$

The pBRDF model is described by two components: diffuse component D_{HS} and the specular component S_{HS}. The former is dependent on the total hemispherical reflectance of a perfect reflector with same surface characteristics ($S_{\mathrm{HS,PR}}$). Parameter M_{00} is the upper left corner element of the Mueller matrix $\boldsymbol{M}$, which replaces the Fresnel coefficients. Here only one element of the Mueller matrix is used, because the detector collecting the reflected light is polarization insensitive and the polarized incident light is described by an appropriate matrix within $\boldsymbol{M}$ [9]. Parameter β is the incident angle with respect to the micro facet normal. Parameter r is a scaling parameter used for fitting. The rest of the symbols are described in table 1.

3. Results

The aforementioned models are used to create a fit for the measured BRDF values. With the T–S model, surface roughness, imaginary part of the complex refractive index, and weights for diffuse and specular components are free parameters to be optimized for the best fit. In the case of anodized surfaces the real part of the refractive index is also fitted. With the pBRDF model the weights for the diffuse and specular components are replaced with a single weight, since the ratio between the diffuse and specular components is fixed as seen in (3)–(5).

The surface roughness profile measurements are used to calculate the root mean squared slope of the surface profile R_{dq}. The R_{dq} value is used in the Beckmann distribution [4] for calculating the micro facet orientation probability distribution for the models. The measured values for the R_{dq} are 0.15 and 0.34 for plain aluminium and anodized aluminium surfaces, respectively. Despite the availability of the measured values, the surface roughness is kept as a free parameter in the model, since the measured value may not be a suitable representation for the whole surface. However, the fitted values for the surface roughness are similar to the measured values within 10%. The refractive index for the plain aluminium surfaces is taken from [11].

The fit is optimized by minimizing the sum of squared residuals weighted with normalized squared reciprocal uncertainty of the measured value. The goodness of fit is described by

$$R^2 = 1 - \frac{\sum_i (x_{f_i} - x_{m_i})^2 w_i^2}{\sum_i x_{m_i}^2 w_i^2}, \tag{6}$$

where x_{f_i} is the fitted value, x_{m_i} is the measured value and w_i is the weight used.

Measurement results and corresponding fitted values with both the T–S model and pBRDF model for the plain roughened aluminium surfaces are seen in figures 2(*a*) and (*b*), respectively. The differences between measured and calculated values are within 1% near the specular peak and reach up to 100% at viewing angles far from the specular peak.

Measurement results and corresponding fitted values with both the T–S model and pBRDF model for anodized roughened aluminium surfaces are seen in figures 3(*a*) and (*b*), respectively. The relative differences between the measurement results and modelled values range from 1% to 100%.

The relative expanded uncertainty ($k = 2$) of the BRDF measurement results is ranging from 2% near the specular peak to 10% at viewing angles far from the specular peak.

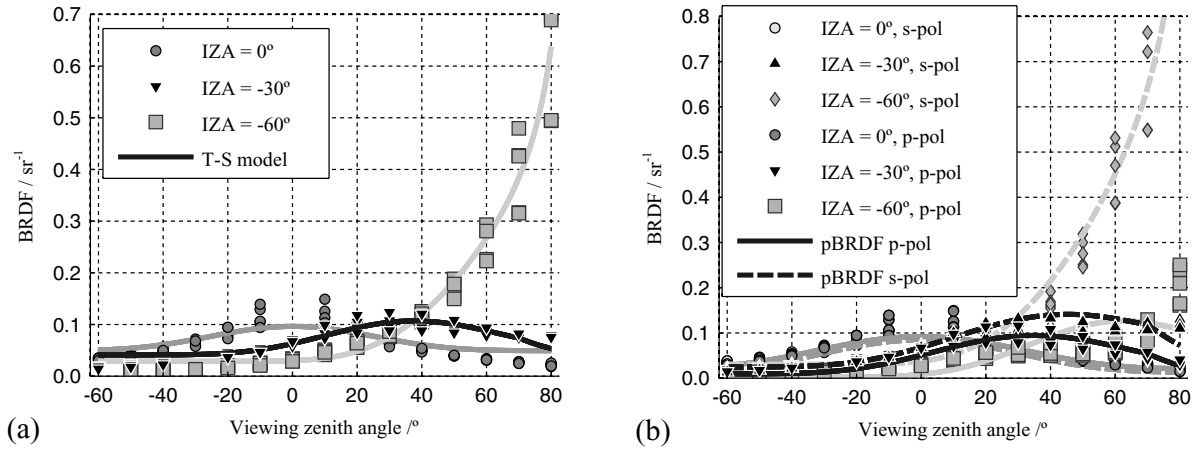

Figure 3. Measurement results of five anodized aluminium surfaces and calculated curves for one surface by (*a*) T–S model, $R^2 = 0.996$, and (*b*) pBRDF model, $R^2 = 0.984$.

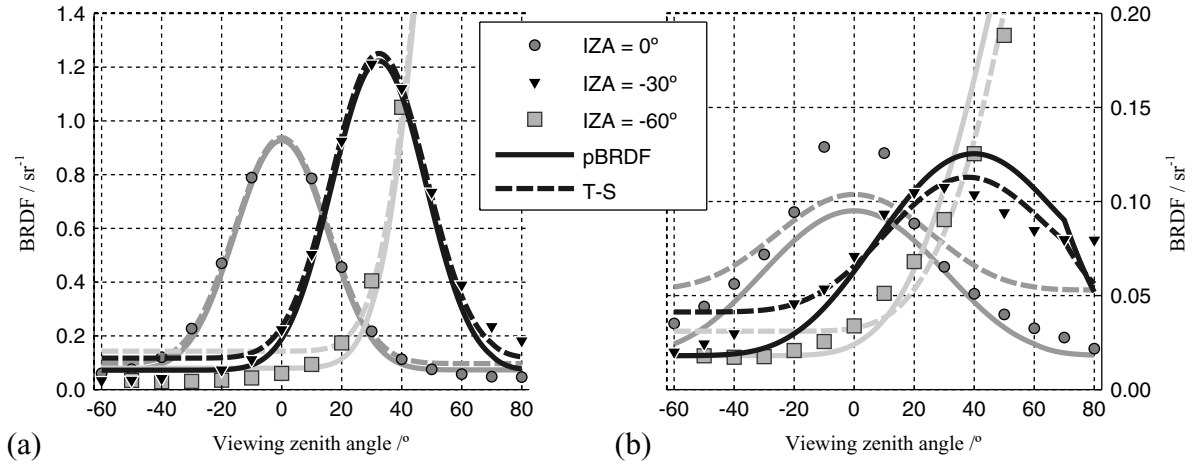

Figure 4. Detailed comparison of fitted models to the BRDF measurement results of (*a*) plain aluminium surface and (*b*) anodized aluminium surface.

4. Discussion

The T–S and the pBRDF can be used as a model for the plain aluminium surfaces, since the deviations from the measured values are close to or within the measurement uncertainties at angles where the level of measured signal is high and therefore uncertainty of the measurements is small. At geometries where the level of measured reflectance is low, the deviations are much larger as seen in figure 4(*a*). The fit may be improved for high viewing zenith angles by adjusting the weights in the optimizing function (6), however this results in deteriorated fit near the angles of specular reflection.

The relative deviations are in a similar range for the anodized surfaces as for plain surfaces for both models as seen in figure 4, but the relative deviations are much smaller at high reflectance levels for the plain aluminium surfaces. The pBRDF model gives a better fit near the angles where the signal level is low, while the T–S model fits better where signal values are higher. For the anodized aluminium surface near zero viewing angle, with IZA $= 0^\circ$, the measurement results can be described by neither of the models.

The large deviation between the measured and the fitted values at large viewing angles and low reflectance levels for non-anodized surfaces may indicate that the Gaussian micro facet distribution (Beckmann distribution) is not an appropriate approximation for these surfaces. Although, in addition to the Gaussian function, Cauchy and Voigt functions were used, no better fit was obtained. Other micro facet distributions may be developed for the BRDF models based on results of improved surface roughness measurements.

The deviations between the fitted values and the measured values for the anodized surfaces, especially near the specular reflection angle for measurements where the incidence angle is 0°, indicate that these models need to be improved for use with these kind of surfaces. Additions such as multilayer scattering and absorption according to Kubelka-Munk theory [12] could be tested.

The relatively large spread (about 30%) in the measured values over different surfaces indicates that in order to use the fitted models reliably, the model parameters need to be obtained for each individual surface separately or averaged over a large sample pool. The large variety in the BRDF values would thus also require an increased amount of modelling work with the RT code validation artefacts consisting of several small cubes [2]. It is not known if natural targets exhibit similar

surface variability, but some light may be shed on this question in the near future [13].

5. Conclusions

The BRDF values predicted by the T–S and the pBRDF models are in a reasonably good agreement with the measurement results for plain aluminium surfaces. For anodized surfaces further development of the model is needed. A major source of uncertainty for the SI traceable validation of RT codes thus may be the choice/relevance of the scattering distribution models used in the setup of the environments for which RT simulations are to be generated.

Acknowledgments

The authors thank Antti Lassila, Asko Rantanen, Björn Hemming, Monika Lecklin, Ilkka Palosuo and Pasi Laukkanen for manufacturing and dimensional characterization of the samples. This work was funded through the European Metrology Research Program (EMRP) project Metrology for Earth Observation and Climate. The EMRP is jointly funded by the EMRP participating countries within EURAMET and the European Union.

References

[1] Clough S A, Shephard M W, Mlawer E J, Delamere J S, Iacono M J, Cady-Pereira K, Boukabara S and Brown P D 2005 Atmospheric radiative transfer modeling: a summary of the AER codes *J. Quant. Spectrosc. Radiat. Transfer* **91** 233–44

[2] Bialek A, Greenwell C, Jaanson P, Chunnilall C, Fox N, Gergely M and Widlowski J-L 2014 SI traceable validation of radiative transfer codes *Proc. NEWRAD 2014 (Espoo, Finland)* pp 63–4

[3] Sparrow E M, Torrance K E and Birkebak R C 1967 Theory for off-specular reflection from roughened surfaces *J. Opt. Soc. Am.* **57** 1105–14

[4] Cook R and Torrance K 1982 A reflectance model for computer graphics *ACM Trans. Graph.* **1** 7–24

[5] Hyde M W, Schmidt J D and Havrilla M J 2009 A geometrical optics polarimetric bidirectional reflectance distribution function for dielectric and metallic surfaces *Opt. Express* **17** 22138–53

[6] Govaerts Y 1996 A model of light scattering in three-dimensional plant canopies: a Monte Carlo ray tracing approach, Space Applications Institute, JRC, (report EUR 16394 EN)

[7] Nevas S, Manoocheri F and Ikonen E 2004 Gonioreflectometer for measuring spectral diffuse reflectance *Appl. Opt.* **43** 6391–9

[8] Blinn J 1977 Models of light reflection for computer synthesized pictures *ACM SIGGRAPH 1977 Proc. (San Jose, California, USA)* pp 192–8

[9] Bass M, Enoch J M, Stryland E W and Wolfe W L 1995 *Handbook of Optics* vol 2 (New York: McGraw–Hill) p 22.10

[10] Priest R G and Gerner T A 2002 Polarimetric microfacet scattering theory with applications to absorptive and reflective surfaces *Opt. Eng.* **41** 988–93

[11] Rakić A D 1995 Algorithm for the determination of intrinsic optical constants of metal films: application to aluminum *Appl. Opt.* **34** 4755–67

[12] Yang L and Kruse B 2004 Revised Kubelka–Munk theory: I. Theory and application *J. Opt. Soc. Am.* A **21** 1933–41

[13] Lolli L, Pisani M, Rajteri M, Santiano M, Widlowski J L, Bialek A, Greenwell C and Fox N 2014 A handheld leaf goniometer for *in situ* spectro-directional measurements *Proc. NEWRAD 2014 (Espoo, Finland)* pp 33–4